PCCP

Accepted Manuscript

ROYAL SOCIETY OF CHEMISTRY

www.rsc.org/pccp

Physical Chemistry Chemical Physics

Dynamic Article Links ▶

ARTICLE TYPE

Facile Synthesis of Exfoliated Co-Al LDHs/Carbon Nanotubes Composite with High Performance as Supercapacitor Electrode

Lei Yu,[a] Nannan Shi,[a] Qi Liu,*[a] Jun Wang,*[a,c] Bin Yang,[a] Bin Wang,[a] Huijun Yan,[a] Yanbo Sun[b] and Xiaoyan Jing[a]

A novel sandwich-like structured Co-Al LDHs/Carbon Nanotubes(CNTs) composite has been successfully synthesized by the elegant combination between exfoliated Co-Al LDHs nanosheets and modified CNTs, which achieved through electrostatic assembly method. It is worth noting that negatively
10 charged the CNTs, sandwiched between the positively nanosheets via the electrostatic force, can not only expand the area of contact of electrolyte ions but also highly improve the conductivity. The as-prepared Co-Al LDHs/CNTs composite exhibited a high specific capacitance of 884 F/g and good cycle stability over 2000 cycles. Therefore, such a facile synthetic route to fabricate the layered structure composite may open a new strategy to prepare other composite with largely enhanced electrochemical properties, which
15 can be of great promise in energy storage device application.

1. Introduction

Two-dimensional (2D) nanosheets are ultrathin and infinite planar functional materials. Due to the special structure of 2D materials, they have remarkably electrical, mechanical and
20 thermal properties.[1-4] Since preparation of graphene had been widely developed as a rapid and simple method, the methodology in preparing ultrathin layers has also been used to explore other two-dimensional materials, for example, the transition metal dichalcogenides (TMDs) and transition metal oxides (TMOs)
25 nanosheets produced by liquid exfoliation of layered materials.[5-9] In addition, there are a lot of other ways to synthesize 2D nanosheets. For example, the nanosheets can be prepared by mechanical cleavage and sonication in an appropriate solvent. Need to mention, nanosheets which are prepared through the
30 exfoliation process have advantages over other routes due to its simple operation and mild conditions.[10-15] Also, this method provides a colloidal suspension of ultrathin nanosheets of high quality and yield.[16, 17]

Layered double hydroxides (LDHs) are typical two-
35 dimensional (2D) nanomaterials. And Co-Al LDHs, with divalent Co^{2+} ion and trivalent Al^{3+} ion, are one of the most commonly studied LDHs because of their excellent electrochemical properties and low cost.[18-20] In recent studies, the problem that LDHs always stacked together and maximized the utility of Co-
40 Al LDHs has been solved by exfoliation.[16] However, because of the bad chemical stability and electron transfer efficiency of exfoliated Co-Al LDHs, Co-Al LDHs cannot fully play their roles in electrochemistry. Thus, nanostructured carbon materials, including carbon nanotubes (CNTs) and graphene, have been
45 considered as intercalation materials to improve the chemical stability and conductivity.[4, 21-23]

Different from 2D LDHs materials, Carbon Nanotubes (CNTs) are one-dimensional (1D) inorganic materials. Due to their good mechanical properties, electrical properties and thermal
50 conductivity properties, CNTs are widely used to assemble nanocomposites, which significantly improve the performance of every matrix material.[24-27] In particular, LDHs and CNTs can form a kind of high performance hybrid composite with both the advantages of the two materials.[28, 29] Linghao Su *et al.* have
55 reported that the multiwall carbon nanotubes compound with Co-Al LDHs improved the electrode stability and enhanced ion/charge transport properties between Co-Al LDHs electrode and electrolyte interface.[28]

Herein, we report a novel strategy for fabricating a sandwich-
60 like composite for application as a pseudocapacitor. The composite is prepared via electrostatic assembly of Co-Al LDHs nanosheets and CNTs. Firstly, the positively charged Co-Al LDHs nanosheets were obtained by intercalation reactions using formamide as intercalated molecules. Then, the surfaces of the
65 positively charged nanosheets were adsorbed by the modified negatively charged CNTs via electrostatic assembly, forming a chemical stability and high electrochemical performance composite.

2. Experimental

2.1 Materials and Chemicals

Cobalt chloride ($CoCl_2•6H_2O$), aluminum chloride ($AlCl_3•6H_2O$), and urea were purchased from Sinopharm Chemical Reagent Co., td. Formamide and other chemicals were purchased from Tianjin Yaohua Chemical Reagents Co. All the chemicals were of
75 analytical grade and were not purified further before use.

2.2 Synthesis and Exfoliation of Co-Al LDHs Nanosheet

In a typical process, cobalt chloride, aluminum chloride and urea were dissolved in 80 mL of deionized water to give the final concentrations of 10, 5, and 35 mM, respectively. And the mixed solution was magnetically stirred for 2 h at room temperature. Then the resulting mixture was transferred into a 100 mL Teflon-lined stainless steel autoclave. The autoclave was sealed and heated at 120 ^{o}C for 8 h. Finally, the pink precipitate (Co-Al LDHs) was collected by centrifugation, washed with deionized water and ethanol several times, and dried completely at 60 ^{o}C.

Typically, 50 mg as-prepared Co-Al LDHs was added respectively in a 50 mL 5 M NH_4Cl, NH_4NO_3, $NaNO_3$ and 50 mL 25 ω% tetramethylammonium hydroxide aqueous solution, which was shocked for 12 h in order to complete the decarbonation. The precipitate was also collected by centrifugation. Then, 50 mg the Co-Al LDHs prepared in the previous step were dispersed in 50 mL formamide and shocked at a speed of 160 rpm for 2 d. Finally, the resulting pink and translucent colloidal suspension was further treated by centrifugation at 2000 rpm for 10 min to remove the unexfoliated parts of LDHs. These processes were finished at room temperature.

2.3 Modification of CNTs

Negatively charged CNTs (CNT-COONa) were prepared according to the modified Salzmann's method.[30] Firstly, CNTs were ultrasonicated for 30 min and refluxed in 9 M HNO_3 at 100 ^{o}C for 12 h. After cooling to room temperature, they were vacuum-filtered through a 0.22 μm Millipore PTFE membrane, and washed with deionized water until the filtrate was neutral, and dried at 60 ^{o}C for 24 h. Then, the obtained oxidized CNTs were added in 4 M NaOH aqueous solution under nitrogen at 80 ^{o}C for 8 h. The resultant (denoted as CNT-COONa) were filtered and washed by deionized water thoroughly until the filtrate was neutral and then dried at 60 ^{o}C for 24 h.

2.4 Assembly of Co–Al LDHs Nanosheets and CNTs

The Co-Al LDHs and CNTs suspension liquid (1 mg/mL) were prepared by adding 50 mg of Co-Al LDHs (after pretreatment) and CNTs (after modification) samples into 50 mL of formamide. The two suspension liquids were added quickly into erlenmeyer flask and shocked at a speed of 160 rpm for 2 d. After sedimentation, the Co-Al LDHs/CNTs composite was formed.

2.5 Characterization

The crystallographic structures of the obtained samples were performed by an X-ray diffraction system (XRD, Rigaku TTR-III) equipped with Cu Kα radiation (λ=0.15406 nm). The microstructure of the products was investigated by the scscanning electron microscopy (SEM, JEOL JSM-6480A microscope) and transmission electron microscopy (TEM, Philips CM 200FEG, 160 kV). X-ray photoelectron spectroscopy (XPS) measurements were performed using a PHI 5700 ESCA spectrometer with monochromated Al KR radiation (hυ=1486.6 eV). All of the XPS spectra were corrected by the C 1s line at 284.5 eV.

2.6 Preparation of Electrodes and Electrochemical Characterization

The electrochemical performances of all the samples were investigated in a three electrode configuration. The working

electrodes were fabricated as follows. A mixture of active material, graphite, acetylene black, and poly (tetrafluoroethylene) (PTFE) at a weight ratio of 85:10:5 was pasted on nickel foam as working electrode with an area of 1 cm^2 and dried at 80 ^{o}C for 12 h in air. The cyclic voltammogram (CV) was tested in a voltage window between 0~0.6 V, and the galvanostatic charge-discharge (CD) was measured between 0~0.5 V. Electrochemical impedance spectroscopy (EIS) was performed in the frequency range from 100 kHz to 5 mHz at the open circuit voltage with a 5 mV disturbing signal. All electrochemical measurements were carried out by a CHI 660D electrochemical work station in 2 M KOH electrolyte.

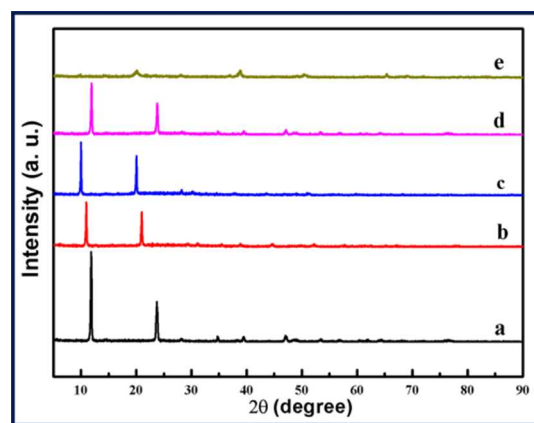## 3. Results and Discussion

3.1 Material Characterization

The crystallinity of the as-prepared Co-Al LDHs samples before and after exfoliation was characterized by XRD. Because the preparation of Co-Al LDHs is using urea as alkali source, the interlayer anion is CO_3^{2-}. However, CO_3^{2-} is very difficult to be displaced by a normal anion-exchange manner because of this exceptionally high affinity to LDHs.31 Such being the case, the pretreatment of decarbonation using other anion such as NO^{3-} or Cl^- is necessary. Fig. 1 shows the XRD patterns of all samples

before(a) and after pretreatment with NH_4Cl(b), NH_4NO_3(c), $NaNO_3$(d) and tetramethylammonium hydroxide(e) aqueous solution. Compared with the as-prepared Co-Al LDHs (Fig. 1a), the peak of Fig. 1c shifts to small angle most obviously. That is to say, after intercalation replace of nitrate ion, the layer spacing increased most obviously. And compared with the pretreatment of $NaNO_3$ (Fig. 1d), ammonium ions can promote the implementation of intercalation replace. The tetramethy-lammonium hydroxide (Fig. 1e) makes Co-Al LDHs produce a chemical reaction to obtain the heterogenite. Fig. 2 shows the XRD patterns of the samples after every treated step. Fig. 2b was tested after pretreatment of NH_4NO_3 aqueous solution. After shaking in NH_4NO_3, the (003), (006) peaks of the prepared samples shift obviously to smaller angle. The interlayer CO_3^{2-} is converted to NO_3^- and the interlayer spacing expands from 0.745 nm to 0.884 nm. So the product has better swelling delamination behavior. As shown in Fig. 2c, the feature diffraction peaks of hydrotalcite disappear after shaking in formamide. The layer structure is destructed and the single nanosheets are got, which can be well observed from illustrations in the Fig. 6. After the assembly of modified CNTs and nanosheets, the (003), (006) peaks appears, but lower than before. The SEM and TEM images of the Co-Al LDHs/CNTs composite in Fig. 3 and 4 provide evidence about this opinion.
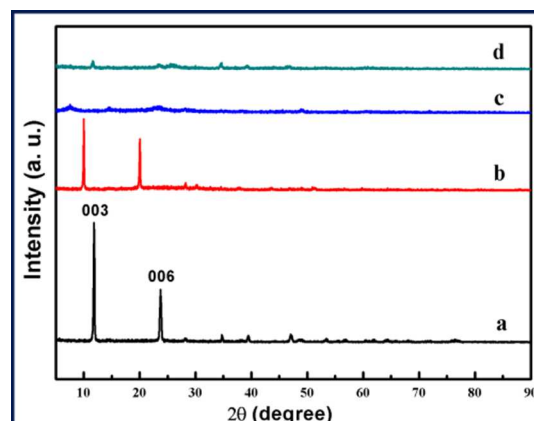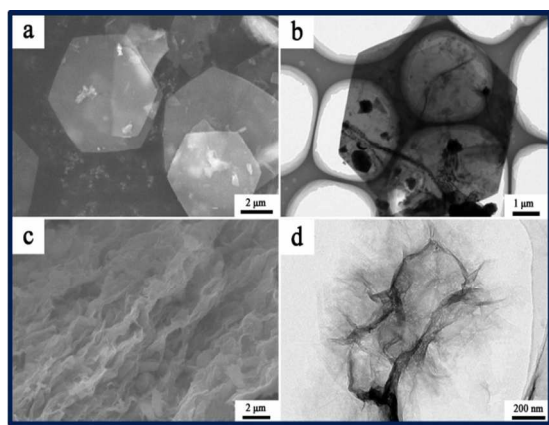

Fig. 3 The SEM and TEM images of the samples before(a, b) and after (c, d) exfoliation

The SEM and TEM images of Co-Al LDHs sample are shown in Fig. 3a and b. As can be seen, the sample typically consists of hexagonal platelets with a side length as large as 3~5 μm. The pretreated samples have similar morphology with the original Co-Al LDHs. The SEM image of exfoliated Co-Al LDHs (Fig. 3c) is tested after drying, so these curled nanosheets stack loosely together. TEM image (Fig. 3d) also well shows the ultrathin and wrinkled morphology of Co-Al LDHs nanosheets. Moreover, a lot of ultrathin nanosheets uniformly disperse in the formamide (Fig. S1 in Supporting Information), which forms a colloidal suspension. For exfoliated Co-Al LDHs nanosheets, those are conducive to compositing with other materials.

The surface and internal morphology of the self-assembly of Co-Al LDHs/CNTs composite is shown in the SEM and TEM image in Fig. 4. As shown, The CNTs are inserted between layers, forming an ordered stacking structure. In the crevice of the LDHs/CNTs composite sample (Fig. 4c), we can see a lot of CNTs disperse inside the material, which can be well observed from illustrations in the Fig. 4b and d. The CNTs-COONa between layers not only expands the area of contact of electrolyte ions, but also improves the conductivity. Thus the electrochemical property of Co-Al LDHs/CNTs composite is much better than Co-Al LDHs.
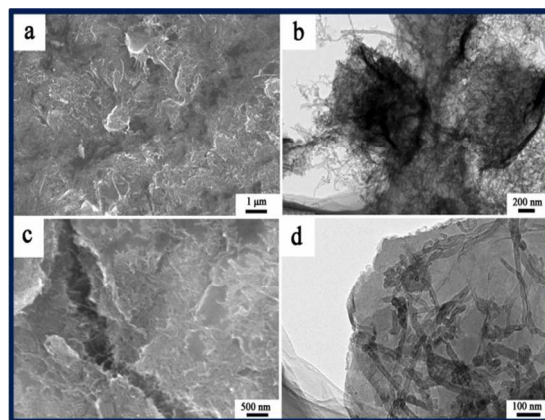

Fig. 4 The SEM and TEM images of the Co-Al LDHs/CNTs composite (a, c) SEM images; (b, d) TEM images.
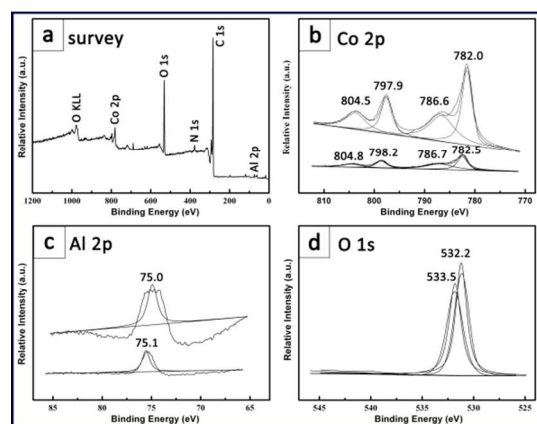

Fig. 5 The XPS spectrum: (a) XPS survey spectrum of the Co-Al LDHs/CNTs composite (b) Co 2p (c) Al 2p (d) O 1s XPS patterns.

To further characterize the chemical composition on the surface of Co-Al LDHs/CNTs composite, XPS spectra analysis of the samples was measured. All elements are calibrated with reference to 284.6 eV of C elements. As is shown in the XPS full spectrum of Co-Al LDHs/CNTs composite (Fig. 5a), the distinct peaks of Co, Al and O elements can be observed within the range of 0-1200 eV. There are not other contaminant species are detectable except the peak of N elements at 398.5 eV. Because the two processes of exfoliation and assembly are carried out in formamide solution. The peak at 398.5 eV is the C-N bond of formamide molecules. It is different for the Co-Al LDHs/CNTs composite to remove the little formamide macromolecular combining with the Co-Al LDHs nanosheets. The Fig. 5b-d are the Co, Al and O fine XPS spectrum of the Co-Al LDHs and Co-Al LDHs/CNTs composite respectively. For the Co-Al LDHs (Fig. 5b), the peaks with binding energy(BE) 797.9 and 782.0 eV are assigned to the Co 2p1/2 and Co 2p3/2.[32] At the relatively high binding energy position, the satellite peaks appear. They are corresponding to the characteristic peaks of Co^{2+}. In the Fig. 5c,

This journal is © The Royal Society of Chemistry [year]

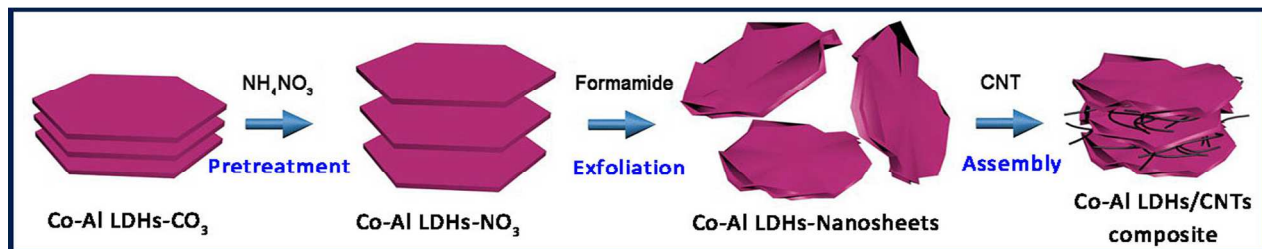*Phys. Chem. Chem. Phys.*, [year], **[vol]**, 00–00 | **3**

Fig. 6 The schematics of each process of assembling exfoliated Co-Al LDHs/CNTs composite.

the fine spectrum of Al 2p displays a peak with binding energy of 75.0 eV, involved the Al^{3+} in the form of Al-OH.[33] As shown in the Fig. 5d, O1s spectrum has only one fitted peak at 532.2 eV, originating from lattice oxygen species. Obviously, the BE of Co2p, Al2p and O1s for Co-Al LDHs/CNTs composite shift to a higher value, as compared to those for Co-Al LDHs. Some literatures have reported the phenomenon.[34-36] The BE shift of elements can be explained by the charge potential model. It is also related to the dispersion, valence and surrounding chemical environment. On this issue in terms of, the increases of composite BE may be due that the positive charges on the Co-Al LDHs nanosheets shift to the CNTs, resulting in reducing of the electron density on the surface of lamella.[35]

The schematics (Fig. 6) well shows all the process of pretreatment, exfoliation and self-assembly. In the first stage, the pretreatment using NH_4NO_3 aqueous solution makes NO_3^- replace CO_3^{2-} in the LDHs interlayer and expands the interlayer spacing, which is in favour of exfoliation. In the second stage, exfoliation process destroys the layers structure and makes Co-Al LDHs form irregular dispersion of nanosheets in formamide. Finally, the formamide solution containing the CNTs-COONa was mixed with the colloidal solution of nanosheets. The self-assembly process was achieved via electrostatic assembly after shaking a period of time, which obtains Co-Al LDHs/CNTs composite with sandwich-like structure.

3.2. Electrochemical Behavior

In order to explore the potential application, electrochemical measurements were made on a three-electrode cell set-up. Fig. 7a shows cyclic voltammetry (CV) curves of the Co-Al LDHs/CNTs composite at various scan rates in the potential range of 0-0.6 V with 6 M KOH as aqueous electrolyte solution. The redox peaks during the potential sweep of the composite corresponded to the reaction of conversion between Co^{2+}/Co^{3+} in the working electrode.[37] With the increasing of scan rate, the specific current of redox peak increases and shows better response relationship. Addition, oxidation peaks and reduction peaks also respectively move towards the positive direction. The shifting direction is small amplitude, but the shape peak remains substantially unchanged, which indicates that the composite has a high rate capability and long cycle life. Fig. 7b shows the CV curves of the LDHs/CNTs composite, Co-Al LDHs and CNTs electrode under the scan rate of 50 mV/s. The differences in the electrochemical properties can be concluded by the areas of CV curves. The area of CV curve and specific current of redox peak of the composite is larger than the area sum of Co-Al LDHs and CNTs, thus the electrochemical propertie of Co-Al LDHs/CNTs composite is
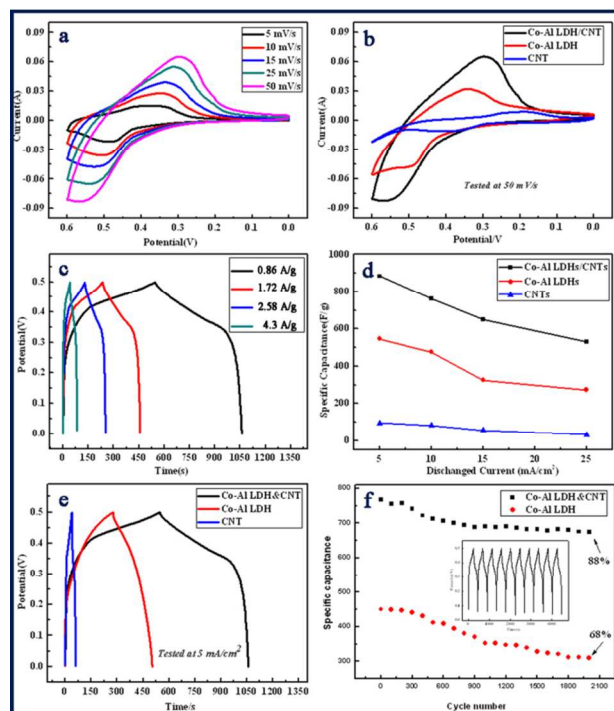
greatly improved.[38, 39]

Fig. 7 The curves of electrochemical measurements: (a,b) cyclic voltammogram curves of the Co-Al LDHs, CNTs and LDHs/CNTs composite; (c,e) galvanostatic charge/discharge measurements; (d) curves of specific capacitance at different current; (f) cycle stability curves

Fig. 7c is the galvanostatic charge/discharge curves of Co-Al LDHs/CNTs composites at different charge/discharge current densities. The specific capacitance of the electrode is calculated by the following eqn (1):

$$C_{sp} = \frac{i \times t}{\Delta v \times m} \qquad \text{.........................(1)}$$

Where $i, t, \Delta v$ and m stand for the constant current density (A/cm^2), charge and discharge time (s), and the potential (V), respectively. As referred to above, when the charge/discharge current is 5, 10, 15 and 25 mA/cm^2 (0.86, 1.72, 2.58 and 4.3 A/g), the corresponding values of specific capacitance is respectively 884, 762, 651 and 529 F/g. Fig. 7d shows the specific capacitance of Co-Al LDHs/CNTs composite, Co-Al LDHs and CNTs electrode at discharge current range from 5 to 25 mA/cm^2. The specific capacitance accompany by significant attenuation behavior. Two reasons can explain this phenomenon: Firstly, with increasing current density, the rate of ion migration required by

4 | *Phys. Chem. Chem. Phys.*, [year], **[vol]**, 00–00

This journal is © The Royal Society of Chemistry [year]

Table 1. Calculated Values of R_S, C_{DL}, R_F, C_{φ}, Z_W and C_L through CNLS Fitting of the Experimental Impedance Spectra Based on the Proposed Equivalent Circuit in Figure 7e

	R_S (Ω)	C_{DL} (F)	R_F (Ω)	C_{φ} (F)	Z_W (Ω)	C_L (F)
Co-Al LDHs	0.3323	0.00702	0.7814	1.219	5.552	1.135
Co-Al LDHs/CNTs	0.3156	0.01115	0.4394	3.999	2.473	1.717

Table 1. Calculated Values of R_S, C_{DL}, R_F, C_{ϕ}, Z_W and C_L through CNLS Fitting of the Experimental Impedance Spectra Based on the Proposed Equivalent Circuit in Figure 7e

the system is increased. Therefore, during a large current discharge, ions and electronic cannot penetrate and ooze quickly from the electrode material in a short time. The active material cannot be fully utilized and the charge-discharge is not complete. In addition, due to the contradiction between the electronic transmission rate and ions diffusion rate, the IR drop increased at higher current densities; as a result the voltage actually involved in the discharge process has become lower. Thus, the attenuation behavior of specific capacitance is obtained.[25]

In the Fig. 7e, the galvanostatic charge-discharge curves of Co-Al LDHs/CNTs composite, Co-Al LDHs and CNTs electrode illustrates clearly the superiority electrochemical properties. When the charge-discharge current is 5mA/cm^2, the specific capacity of Co-Al LDHs and CNTs was 547 F/g and 96 F/g. However, the specific capacity of the LDHs/CNTs composite is much more than the two materials mentioned above and the mixing the Co-Al LDHs and CNTs together, which is illustrated by Fig. 7d, Fig. S2 and Fig. S3 (in Supporting Information).

The cycle stability of Co-Al LDHs/CNTs composites was evaluated by repeating the galvanostatic charge/discharge test between 0 and 0.5 V (vs. SCE) at a current density of 10 mA/cm^2 (1.72 A/g) for 2000 cycles (Fig. 7f). Due to the redox reaction during the charging and discharging, the active sites in the electrode material are consumed. However, the specific capacitance still retains 88% and the average specific capacitance is recorded as 885 F/g after cycling. The cycle life of Co-Al LDHs/CNTs composites is still much better than pure Co-Al LDHs electrode (68% retaining after 2000 cycles). From illustration in the Fig. 7f, each charge-discharge curve has a similar potential response, which also indicates that the charge/discharge process is reversible. This significant cyclic stability of the composites further complements its promise as a supercapacitor material.
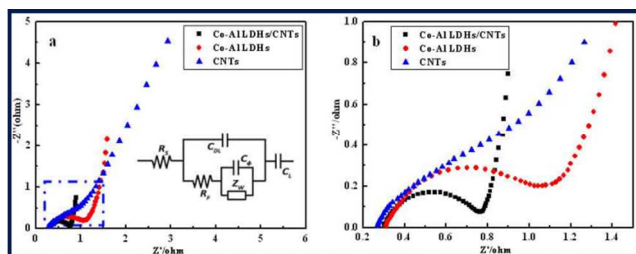

Fig. 8 The electrochemical impedance spectroscopy spectrum: (a) the EIS spectrum of the Co-Al LDHs, CNTs and LDHs/CNTs composite and (b) magnified portion of blue dotted box.

An electrochemical impedance spectroscopy (EIS) is one of the main methods used to characterize the performance of supercapacitors. The EIS data were analyzed by Nyquist plots as shown in Fig. 8a. The EIS curves of these samples are composed of an irregular semicircle in the low frequency region and a slash in the high frequency region. At the low frequencies, the impedance plot theoretically should be a vertical line, which is parallel to the imaginary axis.[29] The slash of Co-Al LDHs/CNTs composites electrode is closer to 90°, which indicates a pure capacitive behavior and a low diffusion resistance of ions in the structure of the composite. At the high frequency region(Fig. 8b), the diameter of the semicircle curve of Co-Al LDHs/CNTs composites is smaller than those of pristine Co-Al LDHs sample and CNTs, which corresponds to a smaller charge transfer resistance (R_F). To analyze further the measured impedance spectra, the complex nonlinear least-squares (CNLS) fitting method based on the equivalent circuit (Fig. 8b) is used. The fitting results are presented in Table 1. In the equivalent circuit, the R_S is bulk resistance of the electrochemical system (the intersection of the curve at real part Z' in the high frequencies range), Z_W is the Warburg impedance (the slope of the curves at a low frequency).[40] Among all the evaluation parameters, the R_S and R_F of Co-Al LDHs/CNT composite are clearly smaller and the C_{DL}, C_{φ} and C_L are larger than that of pristine Co-Al LDHs. The reason is the CNTs between the sandwich-like structure LDHs/CNTs composites structure gives a smaller resistance and higher conductivity. At the same time, it also shows that Co-Al LDHs/CNTs composite is an outstanding supercapacitor electrode material.
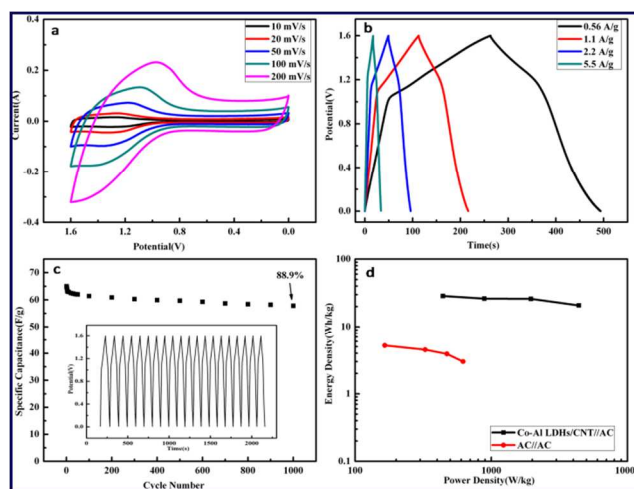

Fig. 9 The curves of electrochemical measurements of asymmetric supercapacitor: (a) cyclic voltammogram curves; (b) galvanostatic charge/discharge curves; (c) cycle stability measurements and (d) Ragone plot related to specific energy and specific power.

This journal is © The Royal Society of Chemistry [year]

Phys. Chem. Chem. Phys., [year], **[vol]**, 00–00 | **5**

In order to explore the application of the Co-Al LDHs/CNTs composite electrode, the asymmetric supercapacitor (named as Co-Al LDHs/CNTs//AC) is successfully assembled. In this system, the positive material is Co-Al LDHs/CNTs composite and negative material is active carbon. The Fig. 9a shows the typical CV curves of the asymmetric supercapacitor at different scan rate (10-200 mV/s). Each curve has a pair of observed oxidation and reduction peaks. The peak current has good response relationship with the change of scan rates. For further evaluating the rate capability of the composite, charge/discharge curves of the asymmetric supercapacitor were tested at different current density. When the current density is 5, 10, 20 and 50 mA/cm^2 (0.55, 1.1, 2.2 and 5.5 A/g), the specific capacitance of Co-Al LDHs/CNTs//AC is respectively 80.6, 73.6 63.8 and 58.4 F/g. As the current density increases from 5 mA/cm^2 to 50 mA/cm^2, the specific capacitance still retains 72.5%, indicating a superior rate of the composite, which is vital factor for electrode material. As higher life-cycle stability is crucial for a supercapacitor, the cycle stability testing of Co-Al LDHs/CNTs//AC was measured using galvanostatic charging-discharging cycles at 20 mA/cm^2(2.2 A/g). Fig. 9c shows that the specific capacitance of asymmetric supercapacitor still retains 88.9% after 1000 cycles. It is worth mentioning that the specific capacitance has dropped to 95.8% after the first 20 cycles and only 6.9% attenuation after the following the cycles. The illustration in Fig. 9d is the first 20 cycles. The similar charge-discharge curve indicates that the asymmetric supercapacitor is reversible, which is ascribed to the high conductivity and large surface area of the composite resulting in better access for the electrolyte into the entire structure. Fig. 9d shows the Ragone plot of the asymmetric supercapacitor measured in the voltage window of 0-1.6 V. The energy density of the asymmetric supercapacitor is 28 Wh/kg at a power density of 444.1 W/kg. As the power density increases, the energy density decline slowly. Comparing with symmetric supercapacitor of activated carbon(AC//AC), the energy density of asymmetric supercapacitor is much higher. Therefore, the asymmetric supercapacitor is expected to be used as an energy supercapacitor.

Conclusions

In conclusion, the Co-Al LDHs/CNTs composite was synthesized by a facile and simple method. An excellent electrochemistry performance as a supercapacitor electrode was achieved: a specific capacitance of 884 F/g and a long cycle life with 88% performance remains after 2000 cycles. The CNTs sandwiched between the two Co-Al LDHs nanosheets not only expand the contact area of Co-Al LDHs nanosheets with electrolyte ions, but also improves conductivity and chemical stability of the electrode material. The results indicate CNTs are always promising nanomaterials with 1D structure. It also shows that Co-Al LDHs/CNTs composites have a great potential for energy storage. For more practical applications, the Co-Al LDHs/CNTs//AC asymmetric supercapacitor was fabricated. The asymmetric supercapacitor present excellent properties, such as high specific capacitance, long cycle stability and high energy density. These encouraging results show the promising applications of the Co-Al LDHs/CNTs electrode in high energy supercapacitors.

Notes and references

[a] *Key Laboratory of Superlight Material and Surface Technology, Ministry of Education, Harbin Engineering University, 150001, P. R. China.*
[b] *State Key Laboratory of Theoretical and Computational Chemistry, Institute of Theoretical Chemistry, Jilin University Changchun, 130023, P. R. China.*
[c] *Institute of Advanced Marine Materials, Harbin Engineering University, 150001, P. R. China.*
* *Corresponding author: Tel: +86 451 8253 3026; Fax: +86 451 8253 3026. E-mail address: zhqw1888@sohu.com†*

1   K. J. Huang, L. Wang, Y. J. Liu, H. B. Wang, Y. M. Liu and L. L. Wang, *Electrochim. Acta*, 2013, **109**, 587-594.
2   J. Feng, X. Sun, C. Z. Wu, L. L. Peng, C. W. Lin, S. L. Hu, J. L. Yang and Y. Xie, *J. Am. Chem. Soc.* 2011, **133**, 17832-17838.
3   A. A. Balandin, *Nature Materials,* 2011, **10**, 569-581.
4   S. Huang, X. Cen, H. D. Peng, S. Z. Guo, W. Z. Wang, T. X. Liu, *J. Phys. Chem. B*, 2009, **113**, 15225-15230.
5   G. H. Han, J. A. Rodríguez-Manzo, C. W. Lee, N. J. Kybert, M. B. Lerner, Z. Q. John Qi, E. N. Dattoli, A. M. Rappe, M. Drndic and A. T. Charlie Johnson, *ACS Nano*, 2013, **7**, 10129-10138.
6   T. Cao, G. Wang, W. P. Han, H. Q. Ye, C. R. Zhu, J. R. Shi, Q. Niu, P. H. Tan, E. G. Wang, B. L. Liu and J. Feng, Nature Commun., 2012, **3**, 887.
7   J. N. Coleman, M. Lotya, A. O'Neill, et al., Science, 2011, **331**, 568-571.
8   H. S. Matte, A. Gomathi, A. K. Manna, D. J. Late, R. Datta, S. K. Pati and C. N. R. Rao, *Angew. Chem.,* 2010, **122**, 4153-4156.
9   M. Fabiane, S. Khamlich, A. Bello, J. Dangbegnon, D. Momodu, A. T. Charlie Johnson and N. Manyala, *AIP Advances*, 2013 **3**.
10   R. Mas-Ballesté, C. Gómez-Navarro, J. Gómez-Herrero and F. Zamora, *Nanoscale*, 2011, **3**, 20-30.
11   M. Z. Cai, D. Thorpe, D. H. Adamson and H. C. Schniepp, J. Mater. Chem. 2012, 22, 24992-25002.
12   Y. Hernandez, V. Nicolosi, M. Lotya1, et al., *Nature Nanotechnology*, 2008, **3**, 563-568.
13   X. C. Dong , W. Huang and P. Chen, Nanoscale Res Lett. 2011, 6, 60.
14   V. Petkov , S. J. L. Billinge, J. Heising, and M. G. Kanatzidis, *J. Am. Chem. Soc.*, 2000, **122**, 11571-11576.
15   Z. Gao, W. L. Yang, Y. X. Yan, J. Wang, J. Ma, X. M. Zhang, B. H. Xing and L. H. Liu, *Eur. J. Inorg. Chem.,* 2013, **27**, 4832-4838.
16   R.Z. Ma, Z. P. Liu, L. Li, N. Iyi and T. Sasaki, *J. Mater. Chem.*, 2006, **16,** 3809-3813.
17   L. Z. Wang , T. Sasaki, Y. Ebina , K. Kurashima and M. Watanabe, *Chem. Mater.*, 2002, **14**, 4827-4832.
18   V. Gupta, S. Gupta, N. Miura, J. Power Sources, 2008, 177, 685-689.
19   Y. Wang, W. Yang, C. Chen, D.G. Evans, *J. Power Sources*, 2008, **184**, 682-690.
20   P.C.K. Vesborg, T.F. Jaramillo, RSC. Advances, 2012, 2, 7933-7947.
21   X. Y. Dong, L. Wang, D. Wang, C. Li and J. Jin, *Langmuir*, 2012, **28**, 293-298.

22 A. Malak-Polaczyk, C. Vix-Guterl and E. Frackowiak, *Energy & Fuels,* 2010, **24**, 3346-3351.

23 L. Wang, D. Wang, X. Y. Dong, Z. J. Zhang, X. F. Pei, X. J. Chen, B Chen and J. Jin, *Chem. Commun.* 2011, **47**, 3556-3558.

24 L. Huang, D. C. Chen, Y. Ding, S. Feng, Z. L. Wang and M. L. Liu, *Nano Lett.* 2013, **13**, 3135-3139.

25 S. W. Lee, J. Kim, S. Chen, P. T. Hammond and Y. Shao-Horn, *ACS Nano*, 2010, **4,** 3889-3896.

26 J. Yang, L. D. Zou, H. H. Song, *Desalination*, 2012, **286**, 108-114.

27 J. Yang, L. D. Zou, N. R. Choudhury, *Electrochimica Acta,* 2013, **91**, 11-19.

28 L. H. Su, X. G. Zhang and Y. Liu, *J. Solid State Electrochem.*, 2008, **12**, 1129-1134.

29 W. L. Yang, Z. Gao, J. Wang, J. Ma, M. L. Zhang and L. H. Liu, *ACS Appl. Mater. Interfaces,* 2013, **5,** 5443-5454.

30 C. G. Salzmann, S. A. Llewellyn, G. Tobias, M. A. H. Ward, Y. Huh and M. L. H. Green, *Adv. Mater.*, 2007, **19**, 883-887.

31 Z. P. Liu, R. Z. Ma, M. Osada, N. Iyi, Y. Ebina, K. Takada and T. Sasaki, *J. Am. Chem. Soc.,* 2006, **128**, 4872-4880.

32 M. Wei, X. Xu, X. Wang, F. Li, H. Zhang, Y. Lu, M. Pu, D. G. Evans and X. Duan, *Eur. J. Inorg. Chem.,* 2006, 2831-2838.

33 Y. F. Gao, M. Nagai, Y. Masuda, F. Sato, W. S. Seo and K. Koumoto *Langmuir*, 2006, **22** 3521-3527.

34 H. Wang, X. Xiang and F. Li *J. Mater. Chem.*, 2010,**20**, 3944-3952

35 G. L. Fan, H. Wang, X. Xiang and F. Li, *Journal of Solid State Chemistry*, 2013, **197**, 14-22.

36 J. Li, S. B. Tang, L. Lu, H.C. Zeng, *J. Am. Chem. Soc.*, 2007, **129** 9401-9409.

37 Z. Gao, J. Wang, Z. H. Li, W. L. Yang, B. Wang, M. J. Hou, Y. He, Q. Liu, T. Mann, P. P. Yang, M. L. Zhang and L. H. Liu, *Chem. Mater.,* 2011, **23**, 3509-3516.

38 F. Li, Q. Tan, D. G. Evans and X. Duan, *Catal Lett.*, 2005, **99**, 151-156.

39 C. J. Jafta, F. Nkosi, L. Roux, M. K. Mathe, M. Kebede, K. Makgopa, Y. Song, D. Tong, M. Oyama, N Manyala, S. W. Chen, K. I. Ozoemena, *Electrochim. Acta*, 2013, **110**, 228-233.

40 B. Wang, Q. Liu, J. Han, X. F. Zhang, J. Wang , Z. H. Li, H. J. Yan and L. H. Liu, *J. Mater. Chem. A*, 2014, **2**, 1137-1143.

41 J. Yan, Q. Wang, T. Wei and Z. J. Fan, *Adv. Energy Mater.*, 2013, **4**, 4

This journal is © The Royal Society of Chemistry [year]

Phys. Chem. Chem. Phys., [year], **[vol]**, 00–00 | **7**